BMC Cancer

RESEARCH

Open Access

UBE2T promotes stage I lung adenocarcinoma progression through PBX1 ubiquitination and PBX1/RORA regulation

Yujie Deng[1,2,3†], Xiaohui Chen[4†], Xuzheng Chen[2,3], Chuanzhong Huang[5], Zhiguang Zhang[2,3], Zhenguo Xu[2,3], Xiurong Wang[2,3], Jiamin Wu[2,3], Li Li[2,3], Jun Song[2,3] and Ruixiang Zhou[2,3*]

Abstract

Background Post-translational modification pathway of protein ubiquitination is intricately associated with tumorigenesis. We previously reported elevated ubiquitin-conjugating enzyme 2T (UBE2T) as an independent risk factor in stage I lung adenocarcinoma and promoting cellular proliferation. However, its underlying mechanisms needed further investigation.

Methods Immunohistochemistry was used to assess the expression of UBE2T and retinoic acid receptor-related orphan receptor α (RORA) in stage I LUAD. Cell proliferation, migration, and invasion of LUAD cell lines were measured by Cell Counting Kit-8 assay (CCK-8), Colony-forming assay and Transwell assay, respectively. Western blot analysis was performed to determine the expression of epithelial-mesenchymal transition (EMT) markers. A xenograft model was established to evaluate the proliferative capacity of UBE2T and its interaction with RORA in promoting LUAD. Mechanistic insights into the promotion of early-stage LUAD by UBE2T were obtained through luciferase reporter assay, chromatin immunoprecipitation and co-immunoprecipitation.

Results UBE2T and RORA expression was significantly up- and down-regulated in early-stage LUAD patients which's proved to be associated with unfavorable outcomes, strengthened cell proliferation, migration, EMT and invasion through its interaction with RORA both in vivo and in vitro. The growth NSCLC xenografts was reduced by down-expression of UBE2T but was suppressed by RORA knockout. Mechanistically, UBE2T mediated the ubiquitination of the intermediate transcription factor PBX1, which played a transcriptional role in downstream regulation of RORA.

Conclusion The oncogenic role of UBE2T and the UBE2T-PBX1-RORA axis in driving malignant progression in Stage I LUAD had been established. UBE2T might be a novel and promising therapeutic target for LUAD treatment.

Keywords Ubiquitination modification, UBE2T, RORA, Progression, Lung adenocarcinoma

†Yujie Deng and Xiaohui Chen contributed equally to this work.

*Correspondence:
Ruixiang Zhou
rxzhou@fjmu.edu.cn
Full list of author information is available at the end of the article

Introduction

Lung cancer remains the leading cause of cancer-related deaths in both sexes in China or worldwide [1–3], contributing mainly to non-small cell lung cancer (NSCLC) histology at a percentage of around 85%. With the prevalence of community-based screening and use of low-dose computed tomography (LDCT), more early-stage NSCLC were diagnosed and surgically treated. However, one notable clinical challenge is the occurrence of local recurrence or distant metastasis in some early-stage NSCLC patients, even shortly after curative treatment. Our previous study identified UBE2T as a potential predictor for worse prognosis in stage I lung adenocarcinoma (LUAD) [4], indicative of a potential tumor promoting factor, and a target for treatment as well. It's demonstrated that dysregulation of UBE2 family member proteins in lung cancer initiates oncogenic signaling pathways, resulting in tumor progression and metastasis [5–7]. UBE2T is one of the key molecules in the UBE2 family that facilitates the transfer of ubiquitin to substrates [8]. In addition to activation of the classical Fanconi anemia (FAN) pathway affecting genome integrity [9], UBE2T also regulated the sensitivity of tumor cells to DNA cross-linked drugs under hypoxic conditions [10].

Retinoid-related orphan receptors (RORs), including family members of RORA, RORB, and RORC, were nuclear receptors and usually regulated by post-translational modifications to maintain their activity and stability. RORA is widely expressed throughout a variety of human organs and tissues including brain and lung [11], exerting its influence on tumor biology through intricate molecular pathways and cellular processes. Furthermore, RORA's been implicated as a melatonergic gene and to play a pivotal role in the transcriptional regulation of genes involving circadian rhythm [12]. The gene regulatory function of RORA's associated with some post-translational modifications like ubiquitination and phosphorylation, in further modulation of the activity and stability of nuclear receptors [13]. Reduced or loss of expression had been reported to be associated with tumor aggressiveness and poor prognosis in breast, colorectal, and lung cancer, indicating its potential role as a tumor suppressor gene (TSG) in these malignancies [14–18]. Results of our preliminary experiment indicated RORA expression was reversely correlated with UBE2T both at an mRNA and protein level. Given the fact that UBE2T was not a canonical transcription factor which could directly bind to the promoter and influence the expression of RORA, we hypothesized that there must be an intermittent substrate or molecule through which UBE2T might probably function to promote the progression of early-stage LUAD.

In the present study, we first verified the high UBE2T expression in early-stage LUAD and its negatively regulation of the downstream gene RORA at both mRNA and protein levels. Then we identified the intermediate transcription factor as *Pre-B-cell leukemia transcription factor 1* (PBX1) which underwent ubiquitination modification by UBE2T and played a transcriptional regulatory role in the upstream regulation of RORA. Eventually we demonstrated the involvement of UBE2T-PBX1-RORA axis in the development and progression of stage I LUAD, providing a novel insight into the underlying mechanisms and prompting a promising therapeutic strategy for early-stage LUAD.

Material and methods

Stage -I LUAD patient samples, tissue microarray and histological analysis

Clinical samples from 43 stage I LUAD patients from Fujian Cancer Hospital between January 2010 and July 2011 were included in this retrospective study. The study protocol was approved by the Human Ethics Review Committee of Fujian Medical University Cancer Hospital (SQ2021-101–01), and a signed informed consent was obtained from each patient. None of the patients had received chemotherapy or radiotherapy prior to surgery, and the final follow-up was updated until death or February 2021. The tissue microarray (TMA) contained formalin-fixed paraffin-embedded (FFPE) samples of 43 LUAD tumors and matched adjacent normal lung tissues. IHC staining was performed on TMA slides via indirect enzyme-labeled antibody method, as described previously [19], using primary antibodies of anti-UBE2T (1:400, ab154022; Abcam) and anti-RORA (1:300, bs-17164R; Bioss), and a secondary antibody (goat anti-rabbit IgG, ZSGB-BIO, China). The immunostaining was evaluated by a semi-quantitative immunoreactive score system (IRS) [20]. The samples were categorized into low and high expression subgroups based on the cut-off value of UBE2T established via X-tile plots [21]. As for result of RORA, only "positive" and "negative" was determined.

Cell lines and culture

Human NSCLC cell lines were obtained from the National Infrastructure of Cell Line Resource. The human bronchial epithelium 16-HBE cells were obtained from the Public Experimental Platform of Fujian Provincial Hospital. All cells have been authenticated by short tandem repeat profiling and were negative for mycoplasma. The cells were cultured in RPMI containing 10% (v/v) fetal bovine serum (FBS) (HyClone: GE Healthcare Life Sciences, Logan, UT, USA) in a 37 ℃ incubator with 5% CO_2.

Plasmids, lentiviral production, and transduction

The lentiviral vectors for UBE2T and RORA overexpression, shRNA, and negative control were purchased from GenePharma (Shanghai, China). A549 and PC9 were seeded into 6-well plates and reached a confluence of 50% ~ 60%, respectively. A549 cells were transduced with the sh-Negative Control and sh-UBE2T lentiviral vector groups, which were constructed for si-UBE2T-192 expression as aforementioned [4], and PC9 with Negative Control and UBE2T overexpression group, following the manufacturer's instructions. Stable UBE2T knockdown and overexpression cell lines were selected using puromycin. The same method was applied for infection with overexpression or sh-RORA lentiviral vectors, G418 was used for screening stable transfection strains. PBX1 and ubiquitin plasmids were purchased from TranSheepBio (Shanghai, China) and transfected into cells using Lipofectamine™ 3000 Transfection Reagent.

Cell proliferation, colony formation and migration assays

Cell proliferation was assessed using Cell Counting Kit-8 (CCK-8) and Colony-forming assays. Cells (5×10^3/ well) were plated in a 96-well plate and incubated for 4-, 8-, 24-, 48- and 72 h. CCK-8 solution (at a concentration of 10%, Vazyme, China) was added to each well and incubated at 37 °C for 1 h. The absorbance was measured at a wave-length of 450 nm using a BioTek ELx800 plate reader. For the Colony-forming assays, transfected A549 and PC9 cell lines were seeded at a density of 1×10^3 cells / well in 6-well plates. The colony-forming units (CFU, consisting of ≥ 50 cells) were observed after 7–10 days. Cell migration capability was determined using the wound-healing assay and non-coated transwell chambers (Corning, USA). 2×10^5 cells /well were seeded in 6-well plates. Once the cells reached approximately 90% confluence, scratch wounds were created using sterile pipette tips. The wounds were photographed at various time points up to 72 h. For the transwell chambers assay, 3×10^5 cells / chambers were seeded. The upper chamber contained serum-free medium, while the lower contained 10% FBS medium as a chemoattractant. After 24 h, the cells that migrated through the chambers were fixed, stained and analyzed.

Western blot

Proteins were collected by RIPA with protease inhibitor PMSF and cocktail (Roche). The total amount of each protein sample was 20 μg, determined by the BCA method (Thermo Fisher Scientific). Samples were loaded onto 8%-20% gradient SDS-polyacrylamide gels (Bio-Rad Laboratories, Inc) and subsequently transferred to polyvinylidene fluoride membrane (PVDF membrane, Millipore). The membranes were incubated with primary antibodies against UBE2T (1:1000, abcam), RORA (1:1000, Thermofisher), Vimentin, E-cadherin, and N-cadherin (1:1000, CST), and Snail-slug (1:1000, abcam) overnight at 4 °C after blocking with 5% (w/v) nonfat milk, then with HRP-linked secondary antibodies (1:3000) at room temperature for 1 h (Zhongshan Company, China). The signals were visualized using enhanced chemiluminescence (ECL) detection (Thermo Fisher Scientific).

RNA-sequencing (RNAseq) and Quantitative real-time PCR (qRT-PCR) analysis

Total RNA was extracted from triplicate samples of A549 cells in the Control and UBE2T overexpression groups using TRIzol reagent (Invitrogen). The concentration, quality, and integrity of the RNA were assessed using a NanoDrop spectrophotometer (Thermo Scientific). Subsequently, sequencing libraries were generated, and RNA sequencing (RNA-seq) analysis was performed on the NovaSeq 6000 platform (Illumina) by Personal Biotechnology Cp. Ltd (Shanghai, China). Differentially expressed genes (DEGs) were analyzed using DESeq (version 1.39.0) with the following criteria: $|\log_2 FC| > 1$ and a significant P-value < 0.05. Heatmaps were created based on the data presented in Supplementary Table 1 (Table S1) and Excel S1. TopGO (version 2.40.0) was utilized for conducting GO enrichment analysis, while ClusterProfiler (version 3.16.1) software was employed to perform the enrichment analysis of KEGG pathways for the DEGs, focusing on the significant enrichment pathway with P-value < 0.05. qRT-PCR was performed using the SYBR® Green Premix *Pro Taq*HS qPCR Kit (Accurate biology, China) to quantify the changes of UBE2T, RORA, and the DEGs. The primers were synthesized by Shanghai Platinum Biotechnology Co., Ltd. The mRNA expression levels were normalized to the level of GAPDH mRNA using the $2-\Delta\Delta Ct$ method. The primer sequences were listed in Table S2.

Luciferase reporter assay

The Luciferase reporter assay was performed using overexpression and small interfering RNA (siRNA) of PBX1. 293 T cells were seeded in a 24-well plate and then transfected with the luciferase reporter vectors and target genes. Additionally, cells were co-transfected with pRL-TK plasmids containing the Renilla luciferase genes which acted as an internal reference gene to establish a consistent baseline for the experiment. After 48 h of transfection, the cells were lysed and the relative activity in each well was measured using the Dual-Lumi™ Luciferase Assay Kit (Beyotime, RG088S).

Chromatin immunoprecipitation (ChIP)

A549 and 293 T cells were fixed in 1% formaldehyde at room temperature for 10 min. Subsequently, after the addition of anti-RNA polymerase, immunoprecipitation was conducted overnight at 4 °C using Normal Rabbit IgG or antibodies specific to the experimental groups. ChIP-Grade Protein G Agarose Beads (CST, 9007, USA) was added to collect immune complexes. The beads were resuspended in elution buffer and incubated at 65 °C for 30 min to release DNA. DNA purification was performed using a spin column and quantified using qRT-PCR (CST, 9004, USA). The ChIP-qPCR products were further validated by agarose gel electrophoresis.

Co-immunoprecipitation (Co-IP)

For Co-IP assay, Specific antibody UBE2T (1:50, abcam179802) and PBX1 (1:50, abcam192606) was initially added to the sample to facilitate an immune complex, which was incubated overnight at 4 °C. Subsequently, the complex was bound to the Pierce™ Protein A/G magnetic beads for 1 h at room temperature. Non-bound material was removed through washing steps. Dissociation of the complex was performed using denaturing conditions by boiling for 10 min at 100 °C with Lane Marker Sample Buffer. Detection of the immunoprecipitated (IP) and input proteins were detected by Western blot analysis (antibody ubiquitin linkage-specific K48, 1:1000, abcam 140,601; Thermo Fisher Scientific, 88,804, USA).

In vivo tumor xenograft models

Approximate 1×10^7 shNC, shUBE2T, or shUBE2T-shRORA A549 cells were injected into the right flank of the 5-6 weeks old male nude mice purchased from the Beijing Vital River Laboratory Animal Technology Co., Ltd (Beijing, China) and housed in the Laboratory Animal Center of Fujian Medical University (Fuzhou, China). All methods related to animals were in accordance with ARRIVE guidelines (https://arriveguidelines.org) for the reporting of animal experiments and a table of Animal Experimental Ethical Inspection (No.: IACUC FJMU 2022–0475) was obtained from FJMU. The tumor size was assessed twice a week lasting for 30 days. Finally, the mice were euthanized (cervical dislocation) 30 days after injection, and the tumors were dissociated, weighed and collected for histological analyses. Tumor volumes were calculated using the formula 1/2 (length × width^2) in mm^3. Specimens were fixed in 4% paraformaldehyde for 12 h, dehydrated with a serial of graded alcohol, cleared with xylene, embedded in paraffin, and subsequently sectioned at a thickness of 4 μm. HE and immunohistochemical staining were performed. Slides were incubated with primary antibodies (UBE2T, 1:400; RORA, 1:200) overnight at 4℃.

Analysis based on public datasets

The transcriptome RNA-Seq raw counts of NSCLC patients were downloaded from TCGA-LUAD [https://portal.gdc.cancer.gov (accessed on 10 August 2024)]. Corresponding genes expression information and clinical information was extracted and merged in R 4.3.1. The downloaded samples were divided into low group and high group with median expression value of UBE2T.

Statistical analysis

The data were presented as the mean ± SEM and analyzed by Student's t-test and one-way analysis of variance (ANOVA) using SPSS software (Version 26.0, Chicago, IL, USA). The correlation between UBE2T expression and clinicopathological parameters of LUAD patients were compared either by independent-sample *t* test, Chi-square or Fisher's exact test. Non-parametric methods such as the Mann–Whitney U test were used instead of the unpaired *t*-test when the data did not meet the normality assumption. Survival was compared by the Kaplan–Meier method with log-rank test, and hazard ratio (HR) and its corresponding 95% credential intervals (CIs) were applied as the effect size and displayed in terms of forest plots. Univariate and multivariate analyses were conducted using the Cox Regression models. The X-tile software program (Version 3.6.1; Yale University School of Medicine, New Haven, USA) and Graphpad Prism 8 (Graphpad Software Inc., USA) were employed. A CIBERSORT method was used for immune infiltration analysis. A Two-tailed $P<0.05$ was considered statistically significant. The above analyses were performed on R (version 4.3.1).

Results

High expression of UBE2T in stage I LUAD correlated with poor clinical prognosis

Analysis of the data from stage I LUAD in The Cancer Genome Atlas (TCGA) demonstrated that the expression of UBE2T was markedly increased in LUAD tissues compared with normal tissues (Fig. 1A, $p<0.001$). Survival analysis revealed shorter overall survival (OS) in stage I LUAD patients with high UBE2T expression (Fig. 1B, $p<0.001$). Immunohistochemistry (IHC) was performed using a tissue microarray (TMA) consisting of 43 pairs of stage I LUAD and adjacent tissues to further assess the clinical significance of UBE2T and RORA. IRS were utilized to distinguish between low and high UBE2T expression, with an IRS of 6 as the cut-off point. Immunostaining of RORA was also

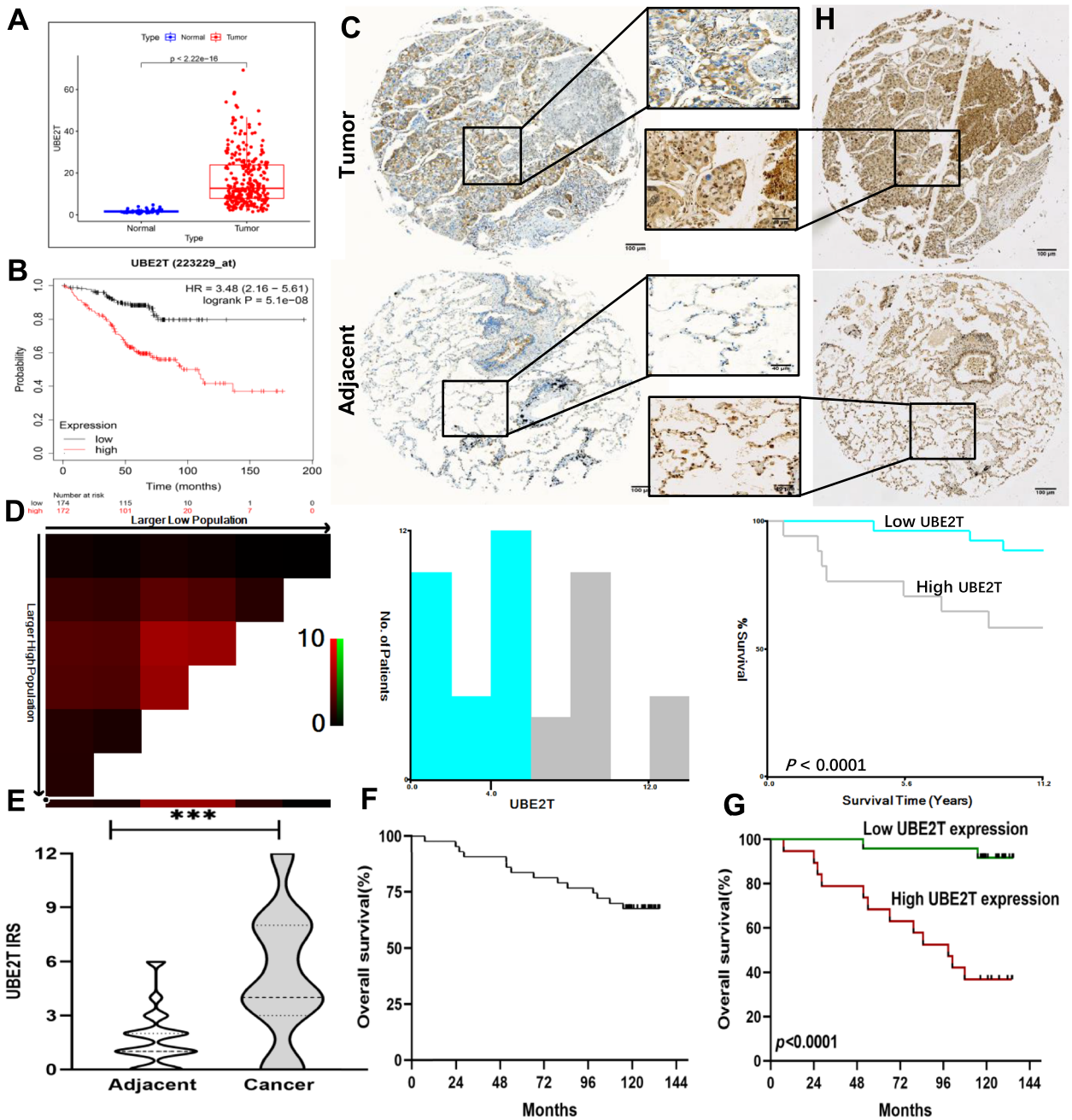

Fig. 1 Highly expressed UBE2T in stage I lung adenocarcinoma (LUAD) was correlated with poor prognosis. **A** The expression of UBE2T in stage I LUAD compared to normal specimen (TCGA), $p < 0.001$. **B** High expression of UBE2T is correlated with shorter overall survival (OS) in stage I LUAD by Kaplan–Meier Plotter database, $p < 0.001$. **C** Representative immunohistochemical staining of UBE2T in LUAD (upper) and adjacent (lower) tissue. Scale bar, 100 μm (4×); 40 μm (10×). **D** Cut-off value of UBE2T (X-tile). IRS of 6 was selected as the cut-off point, classifying samples into low (blue column, IRS ≤ 6) and high UBE2T expression (grey, IRS > 6). **E** The violin plot showing UBE2T IRS in 43 pairs of stage I LUAD (right) and adjacent samples (left), respectively. ($n = 43$, ***$p < 0.001$, paired *t*-test). **F-G** The Kaplan–Meier Plotter curve. OS of the 43 LUAD patients. By the endpoint of follow-up (February 2021),14 patients out of 43 had deceased. The median survival time has not yet been reached (F). The association of UBE2T expression with overall survival was examined by Kaplan–Meier analysis in all 43 LUAD patients. High UBE2T expression compared to low group indicated decreased overall survival with statistical significance ($p < 0.0001$). (G). **H** Representative immunohistochemical staining of RORA in LUAD (right upper) and adjacent (right lower) tissue. Scale bar, 100 μm (4×); 40 μm (10×)

determined for positive or negative. (Fig. 1C-D, 1H). The results showed a significantly higher expression of UBE2T in stage I LUAD compared to adjacent non-cancerous tissues (5.16 ± 0.54 vs 1.72 ± 0.24, $p < 0.001$, Fig. 1C, E). Both survival analysis and clinical characteristics in stage I LUAD TMA indicate the prognostic value of UBE2T. Kaplan–Meier analysis revealed an association between high UBE2T expression and shorter OS ($p < 0.0001$) (Fig. 1F-G). Increased UBE2T expression was closely correlated with clinicopathological features like higher ECOG ($p = 0.031$), larger tumor size (T2a, $p = 0.025$), more invasive predominant growth pattern ($p = 0.028$), and relapse status ($p < 0.0001$) (Table S4). The correlation of RORA with UBE2T had also been evaluated, demonstrating an obvious reverse correlation ($p = 0.033$, Table S3). Furthermore, high UBE2T expression and stage I B were identified as independent prognostic indicators for stage I LUAD patients via univariate and multivariate Cox Regression (Table S5).

UBE2T promoted LUAD cell proliferation, migration and EMT

To investigate the potential biological functions of UBE2T in lung cancer, we assessed UBE2T expression in LUAD cells. The results showed that UBE2T was significantly increased in the A549 and H1299 cell lines compared with the immortalized normal human bronchial epithelial cell line 16HBE ($p < 0.05$), and it was weakest in PC9 cells ($p < 0.01$, Fig. 2A). Based on our previous research [4], we transfected A549 cells with a shUBE2T lentiviral vector (shUBE2T group) or a negative control vector (shNC group), and PC9 cells with a UBE2T overexpression lentiviral vector (UBE2T group) or a negative control vector (NC group). Compared to their control groups, the shUBE2T group showed a significant decrease in the expression level of UBE2T, while the UBE2T group showed enhancement ($p < 0.01$, $p < 0.05$, Fig. 2B). Functionally, the Cell Counting Kit-8 (CCK-8) and colony formation assay demonstrated that the proliferation ability of PC9 cell was enhanced after overexpression of UBE2T ($p < 0.05$, Fig. 2C-D). Wound healing and Transwell assays revealed that upregulation of UBE2T

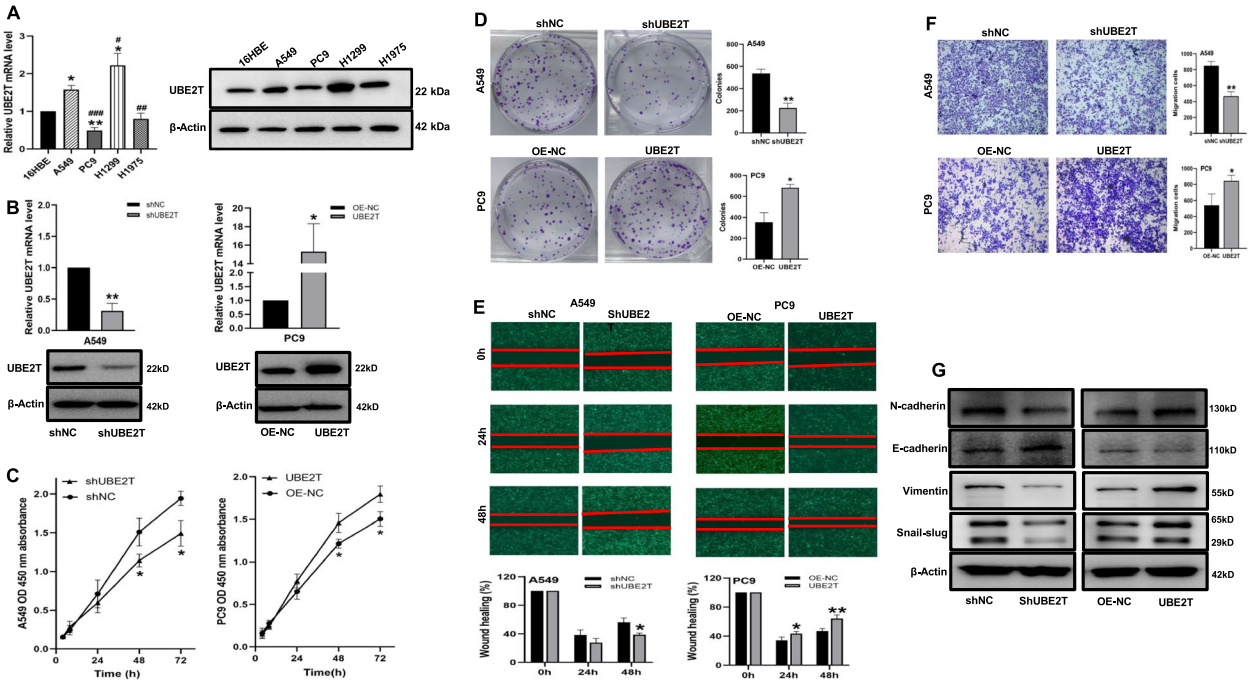

Fig. 2 UBE2T promoted the malignant biological behaviour of LUAD cells. **A** Expression levels of UBE2T mRNA and protein in 16HBE and LUAD cell lines. **B** Verification of UBE2T knockdown/overexpression effects by qRT-PCR and Western blot analyses. **C-D** Assessment of the proliferation ability using the CCK-8 assay (C) and clone formation assay (D) in LUAD cells infected with lentiviral vectors carrying UBE2T gene knockdown or overexpression. Left, A549-shUBE2T/shNC; Right, PC9-OE-UBE2T/OE-NC. Significant reduction colonies of A549 cells transfected with shUBE2T was observed, while an increase was observed in PC9 cells transfected with OE-UBE2T. **E**–**F** Evaluation of cell migration using Wound-Healing (E, 4×) and Transwell Assay (F, 10×) of LUAD cells infected with lentiviral vectors carrying UBE2T gene knockdown or overexpression. UBE2T overexpression significantly promoted cell migration, while knockdown caused suppression. **G** Detection of the effects of UBE2T knockdown/overexpression on EMT downstream target genes by Western blot. *$p < 0.05$, **$p < 0.01$, as compared with 16HBE or NC group; #$p < 0.05$, ##$p < 0.01$, ###$p < 0.001$ as compared with the A549 group, respectively

resulted in a substantial increase in the migration of PC9 cells (Fig. 2E-F). Conversely, downregulation of UBE2T resulted in inhibition of cell proliferation and migration. In addition, we examined EMT-associated markers by WB to confirm whether altering UBE2T mediated the migration and invasion of LUAD cells via EMT. It was observed that overexpression of UBE2T led to a decrease of E-cadherin levels, while an increase in N-cadherin, snail-slug, and vimentin. Conversely, knockdown of UBE2T resulted in the opposite results (Fig. 2G).

UBE2T decreased the expression level of RORA

GSEA analysis indicated high UBE2T expression was significantly enriched in tumor-related pathways like cell cycle (FDR < 0.0001), proteasome (FDR = 0.002), basal transcription factors (FDR = 0.003), oxidative phosphorylation (FDR = 0.015), and ubiquitin-mediated protein degradation (FDR = 0.058) (Fig. S1), demonstrating its close association with ubiquitin-related pathway and an important role in carcinogenesis. To further elucidate the regulatory role of UBE2T in RORs family in LUAD and its possible underlying mechanisms, their correlation was analyzed via GEPIA, indicating a significant negative correlation between UBE2T and RORA, whereas its correlation with either RORB or RORC was much weaker (Fig. 3A). In addition, Spearman correlation analysis from the TCGA dataset including 57 paired stage-I LUAD samples showed a significant correlation between RORA and UBE2T mRNA levels (r = —0.63, $p < 0.05$, Fig. 3B). A significantly negative correlation between the mRNA levels of UBE2T and RORA was also observed among the LUAD cell lines (Fig. 3C). It was found that the transcription level of RORA was significantly increased/decreased upon UBE2T knockdown/overexpression correspondently, as was also verified at protein levels. Taken together, the evidences elucidated that UBE2T might probably regulate RORA expression at both transcriptional and protein level.

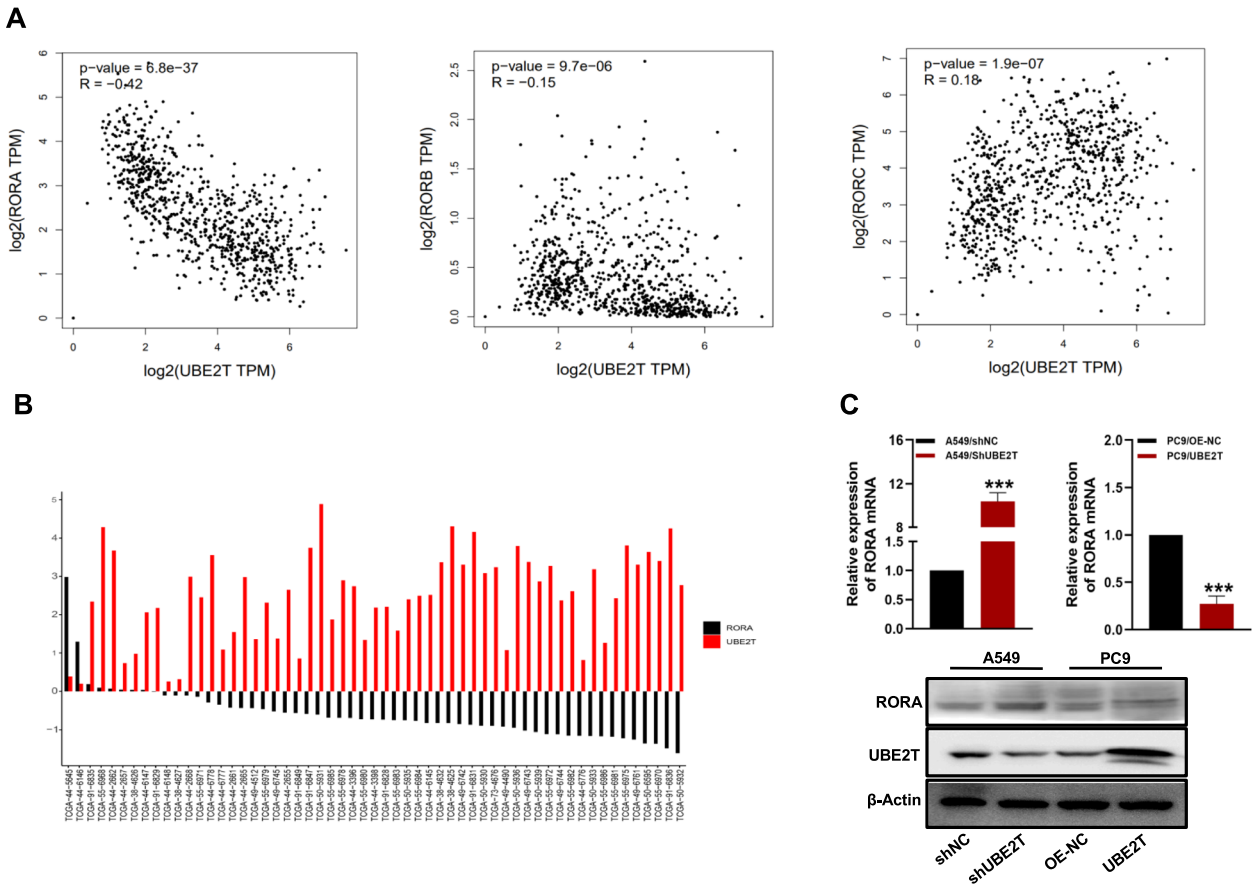

Fig. 3 UBE2T decreases the expression level of RORA. **A** Correlation of UBE2T and RORs family. **B** Fold change of expression and correlation analysis of UBE2T and RORA in 57 paired specimen of stage I lung adenocarcinoma (TCGA). **C** Relative expression of RORA by RT-qPCR and Western blot after UBE2T knockdown or overexpression. ***$p < 0.001$, as compared with NC group, respectively

Transcription factor PBX1's role in the regulation of RORA gene

In order to further investigate the oncogenic mechanisms of UBE2T underlying in early-stage LUAD and the specific negative regulatory role on RORA, we performed transcriptomic sequencing of A549 cell lines transfected with UBE2T and NC vector. Among the genes with transcriptional downregulation that was consistent with the changes in RORA upon UBE2T overexpression in A549 cells, ANXA10, SYT13, EPHA7, ZPLD1, EVA1A, FLRT2, and TNFAIP6 were the top genes with the most significant changes ($|\log_2 FC| > 1.5$, $p < 0.001$) (Fig. 4A-B, Table S1). KEGG enrichment showed pathways related to cancer (Fig. 4C). RT-qPCR validation of the DEGs confirmed that the mRNA expression levels of ANXA10, SYT13, EPHA7, ZPLD1, EVA1A, and FLRT2 were significantly decreased in the A549-OE-UBE2T group compared to the NC group (Fig. 4D).

Since PBX1 was a common transcription factor, covering targeted genes like RORA, EPHA7, FLRT2, EVA1A and SYT13 (Fig. 4E). We then hypothesized that PBX1 might probably be the common transcription factors for the DEGs downstream of UBE2T, as was validated by RT-qPCR. K-M Plotter analysis indicated a tight correlation between high expression of PBX1 and longer OS in stage I LUAD (Fig. 4F). Taken together, we then set out to investigate the potential relationship between the transcription factor PBX1 and RORA using a dual-luciferase reporter assay and ChIP-qPCR, indicating an enhanced luciferase activity on the condition of overexpression of PBX1 and RORA ($p < 0.01$), and a reduction of luciferase intensity upon silencing PBX1 ($p < 0.05$, $p < 0.01$) (Fig. 4G). In the ChIP-qPCR analysis, we investigated the enrichment of PBX1 on the RORA promoter region in 293 T and A549 cells. The ChIP-qPCR primers were designed for the region predicted by the NCBI website as the binding site of PBX1 and RORA (Table S6). Fold enrichment analysis revealed that compared to the IgG group, PBX1 was significantly enriched on the RORA promoter in the IP group, locating at the range of -976 to -996 bp of the transcription start site (TSS) of RORA, with an enrichment fold of approximately tenfold and an enrichment efficiency ranging from 30 to 65% (Fig. 4H). The agarose gel electrophoresis analysis of the ChIP-qPCR products showed that amplified fragments in the ChIP-RORA group was consistent with the predicted

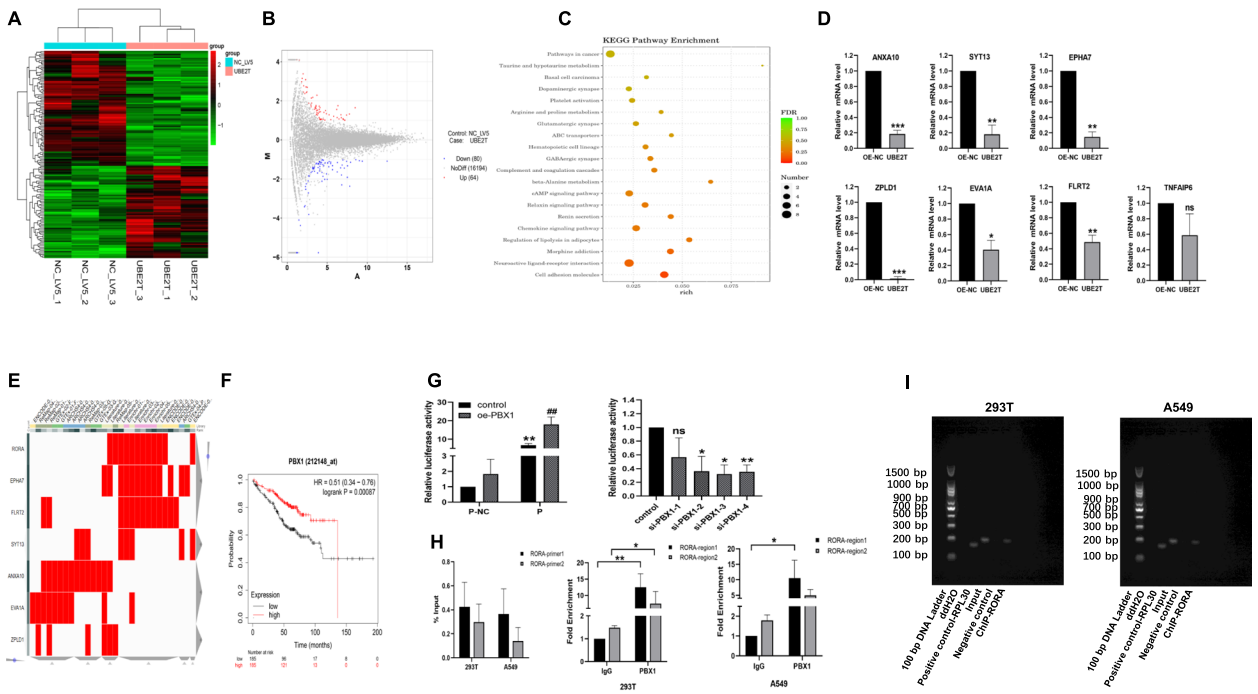

Fig. 4 Common transcription factor PBX1 being predicted by ChEA3 and the binding of PBX1 to the RORA promoter. **A** Hetmap of DEGs after overexpression of UBE2T. **B** MA plot (|logFoldChange| vs average intensity) of DEGs. **C** KEGG pathway enrichment analysis. **D** Relative mRNA level of DEGs measured by RT-qPCR. **E** Clustergram of gene sets and transcription factors PBX1. **F** Kaplan–Meier Plotter analysis of PBX1 in stage I LUAD (Kaplan–Meier Plotter【Lung cancer】). **G** Validation of the binding of PBX1 to the RORA promoter by Dual Luciferase Reporter Assay. **H** Validation by ChIP-qPCR. **I** Agarose gel electrophoresis of ChIP-qPCR products from 293T (left) and A549 (right) cell lines. Positive control-RPL30 (the PCR product was about 161 bp, Lane 3), Input (the target product was about 187 bp, Lane 4), Negative control (Lane 5), ChIP- RORA (the target PCR product was about 187 bp, Lane 6).(100 bp DNA Ladder)

length (primer 1), which also aligned with Input group (F4g. 4I). These findings demonstrated the involvement of PBX1 in the regulation of the activity of RORA promoter. PBX1 was then selected for further analyses due to its downregulation of the RORA promoter in response to UBE2T overexpression.

UBE2T decreased RORA expression by ubiquitinating PBX1, which further transcriptionally regulated RORA

The transcriptional regulatory role of PBX1 on RORA and other downregulated genes in response to the overexpression of UBE2T had been clearly established. In view of the ubiquitination modification function of UBE2T itself, we hypothesized UBE2T would probably affect PBX1 expression via ubiquitination and subsequently demonstrate a transcriptional regulation on RORA.

To clarify the protein degradation pathway of PBX1, LUAD cells were treated with the proteasome inhibitor MG132 and cycloheximide (CHX). The experimental group were treated with CHX (50 μg/ml) at 0, 1, 2, 3, and 4 h, while the control group treated with both CHX (50 μg/ml) and the proteasome inhibitor MG132 (10 μg/ml) at the same time intervals. Results showed that PBX1 protein levels in the control group remained stable, while that in the experimental group treated with CHX alone gradually degraded, with the IC50 values of 2.47 and 3.7 for A549 and PC9 cell lines, respectively, demonstrating PBX1 might have undergone degradation through ubiquitin–proteasome pathway (Fig. 5A). Furthermore, it's also observed that knockdown or overexpression of UBE2T resulted in an inverse correlation with PBX1 levels (Fig. 5B). PBX1 expression was then examined after CHX (50 μg/ml) treatment following UBE2T knockdown or overexpression. In the UBE2T knockdown group, the PBX1 protein exhibited stability with an extended half-life, while the degradation of PBX1 protein was accelerated in the UBE2T overexpression group, with an IC50 value of 2.6 (Fig. 5C). These findings suggested that UBE2T downregulated the expression level of PBX1.

Interaction between UBE2T and PBX1 was then detected by immunoprecipitation. A549 cell lines were lysed, and immunoprecipitation (IP) was performed using UBE2T antibody, and the targeted protein PBX1

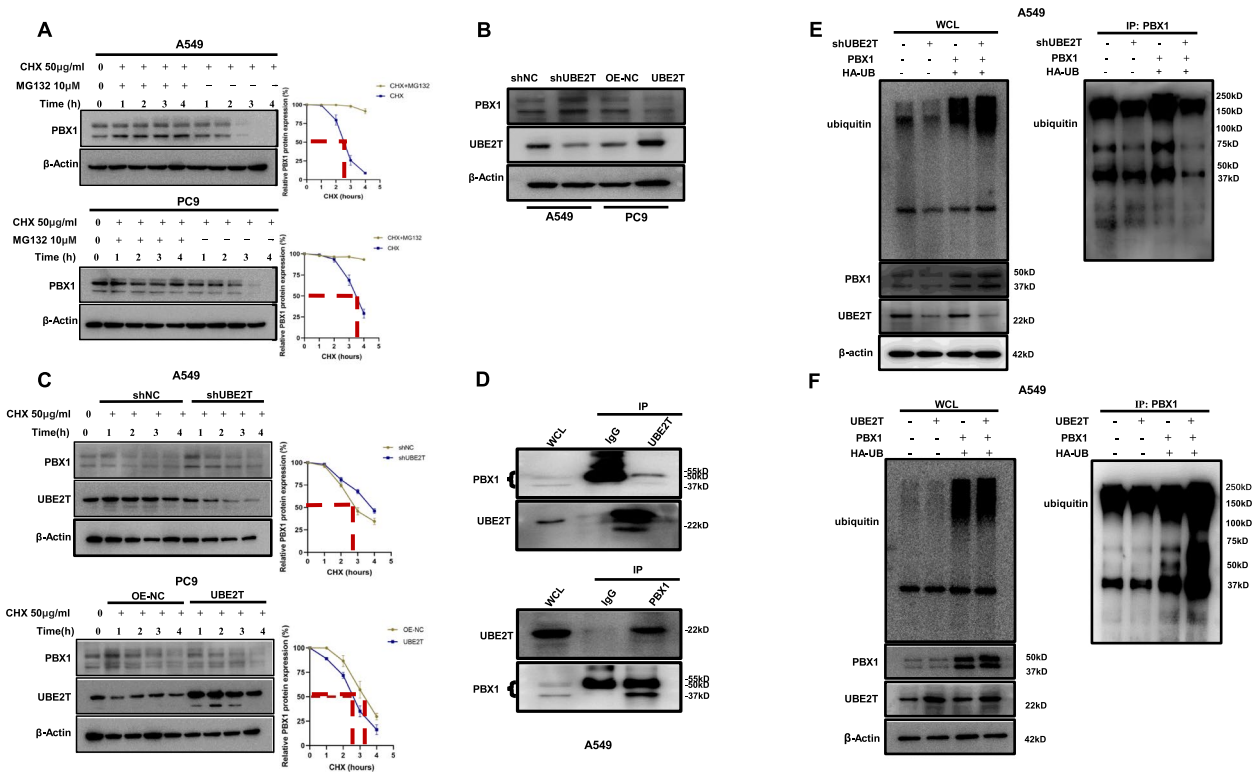

Fig. 5 Interaction between the E2 Conjugating Enzyme UBE2T and its substrate PBX1, and UBE2T-mediated enhancement of PBX1 ubiquitination. **A** PBX1 underwent degradation through the ubiquitin–proteasome pathway. **B** The substrate protein PBX1 was detected following UBE2T knockdown/overexpression. **C** The expression level of PBX1 remained relatively stable in the shUBE2T group after treatment with CHX (50μg/ml) for up to 4 h. **D** Interaction between the E2 Conjugating Enzyme UBE2T and the substrate PBX1 (in vivo). **E–F** Knockdown of UBE2T attenuated the ubiquitination of the substrate protein PBX1 (E) whereas UBE2T overexpression enhanced it (F)

was detected by immunoblotting (IB). It's observed that PBX1 antibody could pull down UBE2T, indicating an interaction between these 2 molecules, and here WCL served as a positive control while IgG as a negative control (Fig. 5D). Exogenous ubiquitin molecules and ubiquitin antibodies were further used to detect the ubiquitination levels of PBX1 in different UBE2T states. OE-PBX1 and HA-UB plasmids were co-transfected into A549-OE-UBE2T cells for 48 h, with a prior treatment of 10 μg/ml MG132 for 4 h before co-transfection termination. Immunoblotting was performed using ubiquitin after immunoprecipitation of the target protein by PBX1**.** Results showed that UBE2T overexpression enhanced PBX1 ubiquitination, which subsequently led to increased degradation of PBX1 protein through the ubiquitin–proteasome pathway. However, knockdown of UBE2T attenuated the PBX1 ubiquitination process, resulting in a sustained level of the PBX1 protein (Fig. 5E-F).

UBE2T promoted the malignant biological behavior of LUAD cell lines through its downstream effector RORA (in vitro)

To validate whether RORA was an essential downstream gene of UBE2T that mediated the function of UBE2T in LUAD, we conducted a rescue assay. A549-shUBE2T cells were transfected with an RORA knockdown vector (A549-shUBE2T-shRORA), while PC9-UBE2T cells were transfected with a RORA overexpression vector (PC9-UBE2T-RORA) (Fig. 6S A), demonstrating that, compared with A549 shNC and shUBE2T group, RORA knockdown reversed the effect on inhibition of cell proliferation caused by UBE2T knockdown (Fig. 6S B-C), as well as migration (Fig. 6S D), and EMT (Fig. 6S E). However, overexpression of RORA rescued the malignant biological behavior of PC9, even if UBE2T was overexpressed (Fig. 6S B-E). Our finds demonstrated that RORA was an essential downstream effector of UBE2T in LUAD.

UBE2T promoted the malignant biological behavior of LUAD through its downstream effector RORA (in vivo)

Tumor xenograft models were established by subcutaneous injection of A549-shNC, A549-shUBE2T, or A549-shUBE2T-shRORA cell lines into BALB/c-nu mice to confirm the results in vivo. Our findings indicated that tumors derived from A549-shUBE2T group resulted in smaller sizes compared with the shNC group, whereas tumors from A549-shUBE2T-shRORA group larger than those from the A549-shUBE2T group (Fig. 6A-B, $p < 0.01$, $p < 0.05$, respectively). Immunostaining demonstrated that UBE2T expression was lower in shUBE2T and shUBE2T-shRORA groups compared to the shNC group (Fig. 6C-D, $p < 0.05$). RORA expression was increased upon deregulation of UBE2T in shUBE2T group ($p < 0.05$), while compared with that in the shUBE2T group, RORA IRS was decreased in the shUBE2T-shRORA group (Fig. 6C-D, $p < 0.05$). In summary, UBE2T promoted the progression of LUAD in vitro and in vivo, and the UBE2T-RORA pathway might play an essential role in initiation and progression of LUAD (Fig. 7).

Analyses based on public dataset

Based on the analysis of TCGA dataset, we found that expression of UBE2T differed significantly in the LUAD patients with different clinical or pathological stages (Fig. 2S A, B). The forest plot demonstrated that high UBE2T expression was closely correlated with female gender, smokers, adenocarcinoma histology, stage I disease, T1 disease, absence of LN involvement (all $p < 0.01$, Fig. 2S C). In addition, when looking into the correlation of UBE2T with immune cells, we found that enhanced expression of UBE2T was positively correlated with macrophage M0/1, resting mast cells, monocytes, activated/resting CD4 memory T cells, CD8 T cells, and helper follicular T cells (all $p < 0.01$, Fig. 2S D).

Discussion

UBE2T was identified as an independent risk factor in early-stage LUAD in our previous study, while no statistical significance had been determined in mid- or late-stage LUAD patients [4]. In the present study, we first confirmed that enhanced UBE2T expression was associated with larger tumor size (T stage), more invasive predominant growth patterns (PGPs), higher probability of recurrence and shorter OS in early-stage LUAD. When further looking into the underlying mechanisms, we then demonstrated that UBE2T promoted LUAD cell proliferation, migration, invasion and EMT through its interaction with RORA both in vivo and in vitro, probably by mediating the ubiquitination of the intermediate transcription factor PBX1 that's believed to play a transcriptional role in the upstream regulation of RORA.

The ubiquitin system is a multi-step cascade process of protein modification that involves ubiquitin, ubiquitin-related enzymes (UBE), and proteasomes to maintain homeostasis in eukaryotes [22]. As a key member of UBE2 family, UBE2T was indicated to maintain genome integrity through the FAN signaling pathway [9], and participate in cell cycle, basal transcription factors, and ubiquitin-mediated proteolysis related to tumorigenesis [23–25]. UBE2T over-expression was found in a wide spectrum of malignancies, including hepatocellular carcinoma [26], head and neck squamous cell carcinoma [24], gastrointestinal tumors [8, 27], breast and ovarian cancer [28–30], glioblastoma [31], and

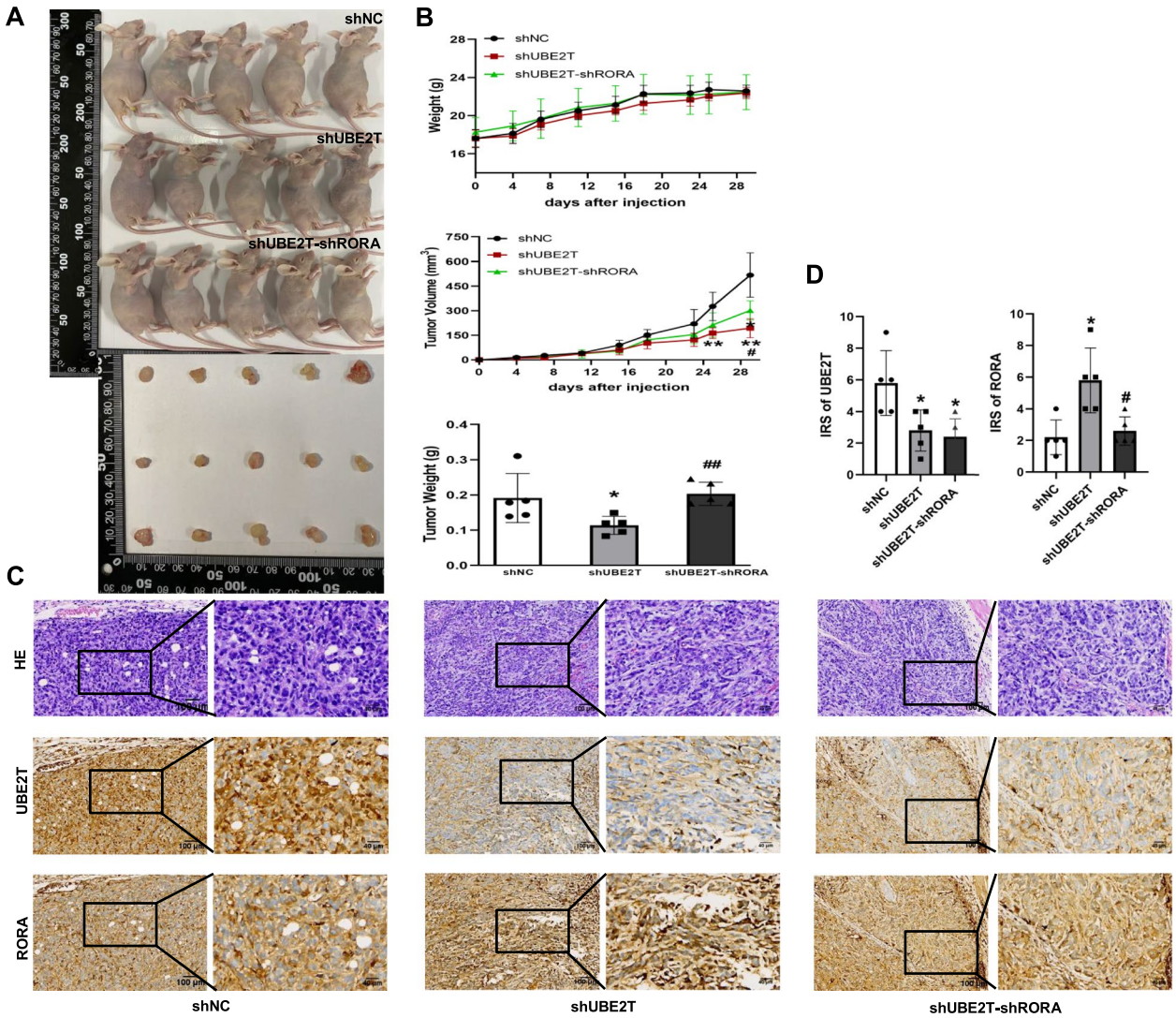

Fig. 6 UBE2T promoted the malignant biological behaviour of LUAD through the downstream effector RORA (in vivo). **A** Representative BALB/c-nu mice bearing tumors after inoculation (Day 30). **B** Measurement and calculation of tumor volumes and weight ($V = 1/2 \times L \times W^2$). **C** HE and IHC in shUBE2T or shUBE2T-shRORA group, compared with shNC group. Scale bar, 100 μm (×10); 40 μm (×40). **D** IRS of UBE2T and RORA in xenograft tumor specimens after UBE2T knockdown or combined with RORA knockdown ($n = 5$). *$p < 0.05$, **$p < 0.01$, as compared with shNC group; #$p < 0.05$, ##$p < 0.01$, as compared with shUBE2T group, respectively

lung cancer as well [23, 32, 33], via signal transduction pathways like GSK3β/β-catenin [34], p53/AMPK/mTOR [35], EMT [36] and so forth. Given all these established facts, UBE2T could be a choice therapeutic target in cancer treatment. Theoretically, targeting the molecule in the upmost stream in UBE2T-PBX1-RORA axis could possibly inhibit or reverse the evolvement of the onset of LUAD, as UBE2T overexpression was demonstrated as an early event in the process of its carcinogenesis. Using a gene-editing technique, we could alternatively weaken the related targets like PBX1 in the axis and inevitably inhibit the malignancy. However, despite its important function, UBE2T was considered as an undruggable target due to lack of a pocket for binding to small molecules with satisfied properties for clinical applications. Anantharajan et al. [37] adopted a high-throughput screening assay and two compounds-ETC-6152 and ETC-9004 containing a sulfone tetrazole scaffold were identified, with confirmative activity of UBE2T blocking. Moreover, Wang and Yu et al. [25, 38] reported that the novel inhibitor of UBE2T, M435-1279, acted inhibit the Wnt/β-catenin signaling pathway hyperactivation through blocking UBE2T-mediated degradation of RACK1, resulting in

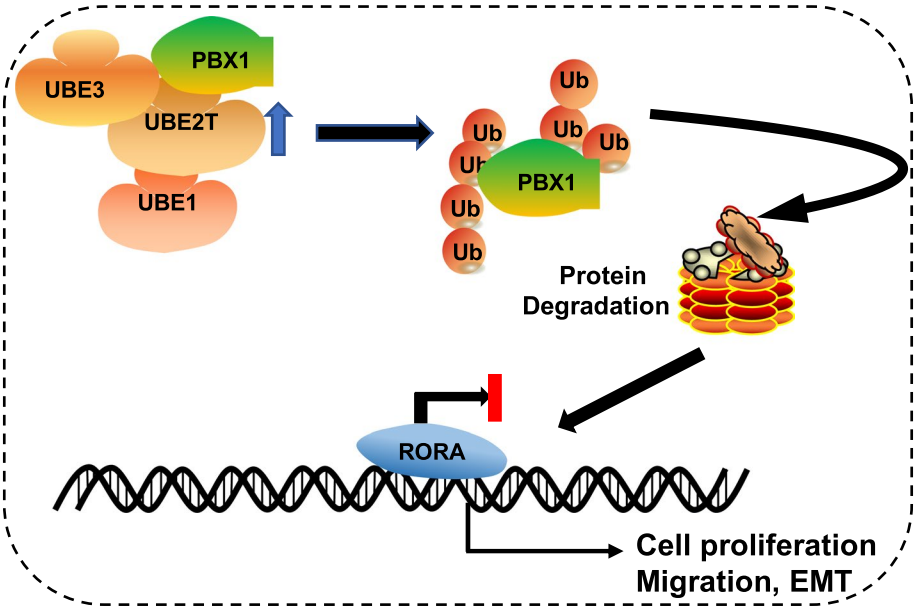

Fig. 7 A diagram of ubiquitination modification of UBE2T to downregulate PBX1/RORA in the development and progression of LUAD

suppression of glioblastoma and gastric cancer progression with lower cytotoxicity in the meantime.

In the bioinformatic analyses, however, we found that overexpressed UBE2T was positively correlated with the congregation of some immune cells, especially monocytes, activated/resting CD4 memory T cells, CD8 T cells and helper follicular T cells, which were main effect cells in correspondence to immunotherapy. We thus hypothesized that although higher UBE2T defined a subgroup of LUAD with unfavorable prognosis, it might possibly simultaneously define the same subgroup with higher potential response to immunotherapy. On the contrary to our demonstration, Pu et al. [33] demonstrated that overexpressing UBE2T could increase PD-L1 expression and inhibit toxicity of CD8 + T cells to LUAD cells. In vivo experiments revealed that UBE2T knockdown hindered tumor growth, inhibited PD-L1 expression, and facilitated CD8 + T cell infiltration. In response to this seemly paradox findings, we pondered it necessary to figure out the exact correlation within tumor immune microenvironment (TIME) and status of UBE2T expression in both patients population and cell lines. In addition, they also verified the role of UBE2T in mediating SORBS3 ubiquitination to enhance interleukin-6/signal transducer and activator of transcription 3 (IL-6/STAT3) signaling and promote LUAD development both in vitro and in vivo [23], demonstrating both PD-L1 and IL-6 could possibly be used as potential biomarkers for selecting patients who were most likely to benefit from therapies targeting the UBE2T pathway. Taken together, UBE2T would hopefully turn out as a potential therapeutic hub triggering tumoricidal activities in terms of different biological mechanisms.

Under normal conditions, E2 enzymes like UBE2T require E3 ligases to confer substrate specificity and facilitate the transfer of ubiquitin to the target proteins. It's observed in our study that knockdown or overexpression of UBE2T resulted in an inverse correlation with PBX1 levels, and PBX1 antibody could pull down UBE2T, demonstrating a tight interaction within these 2 molecules. UBE2T alone could further inhibit PBX1 transcriptional activity and downregulate the PBX1 downstream genes, such as RORA, without the evidence of existence of E3 ligases, as had been demonstrated by us and others [39]. We then hypothesized that there might be circumstances under which UBE2T could ubiquitinate target proteins without E3 ligases, although such scenarios were likely to be rare and not fully understood. Some E2 enzymes was shown to possess intrinsic ubiquitin ligase activity, allowing them to transfer ubiquitin to substrates directly without the need for an E3 ligase. Recently, Tao et al. [31] reported UBE2T functioned as the Ub-enzyme of ribosomal protein L6 (RPL6) and induced the ubiquitination and degradation of RPL6 in an E3 ligase-independent manner through direct modification by K48-linked polyubiquitination, thus contributing to the malignant progression of glioblastoma cells and confirming our hypothesis on the onset of E3 ligase-independent manner. PBX1 (Pre-B cell leukemia transcription factor 1) is a member of the TALE (three amino acid loop extension) class of homeodomain transcription factor, targeting

ubiquitous developmental and organ-specific genes, driving cell proliferation, pluripotency and differentiation by PBX1 alone or by the chimeric E2A-PBX1 protein [40]. PBX1 still plays a role in tumor suppression by inhibiting proliferation, mediating apoptosis and ROS related oxidative damage due to its potential to induce genomic instability and mutations, as well as maintain the functionality of the immune system [41]. Mutations or imbalances in the ubiquitination/deubiquitination signaling pathway in prostate cancer led to abnormalities of the deubiquitinase USP9X, which was also responsible for deubiquitinating PBX1 [41]. This results in abnormality of PBX1 status, contributing to occurrence and treatment resistance [42]. In LUAD, the ubiquitin ligase TRIM26 bound to PBX1, leading to its polyubiquitination and subsequent degradation, which ultimately inhibited its transcriptional activity and promoted cellular proliferation [39]. In our study, however, as a co-transcription factor of downstream-downregulated genes including RORA after UBE2T overexpression, PBX1 was first found to interact with UBE2T, which ubiquitinated and degraded through the ubiquitin–proteasome pathway, bridging the interaction of UBE2T with RORA. Then it's elucidated that PBX1 was involved in ubiquitin-mediated degradation through its interaction with UBE2T in early-stage LUAD, which was further enriched in the understanding of PBX1 ubiquitination in solid tumors. PBX1 forms heterodimer complexes with Hox proteins, or collaborates with transcription factors such as PREP1 and MEIS1 [43] binding to DNA to regulate the target genes. Experimental research revealed that UBE2T negatively regulated RORA, and restoring RORA partially inhibited the malignant phenotype promoted by UBE2T, confirming the inhibitory effect of RORA on the proliferation and migration of LUAD cell lines.

RORA is widely expressed in human body and primarily down-regulated [44]. In the bioinformatics analysis of melatonergic gene and integrative pan-cancer [12], RORA was significantly decreased in LUAD and associated with prognosis. Pathways associated with the anticancer effects of RORα include RORα phosphorylation and transcriptional repression through the Wnt/β-catenin pathway [45], as well as Wnt5α/PKC activation [46, 47], which contributed to the occurrence of EMT [48]. Our study also found that UBE2T promoted EMT via RORA, which ultimately led to tumor invasion and metastasis.

Some limitations in the paper should be mentioned. First, the mechanism of interaction within UBE2T, PBX1 and RORA was only demonstrated in limited cell lines, while whether this mechanism also works in other LUAD cell lines remained unknown. In the future study, more cell lines and more precision techniques like CRISPR-Cas9 for gene editing or RNA interference would be used to confirm the universality and specificity of the current findings. Second, higher grade of evidence in our future work would be needed to further confirm the specificity of the interaction between UBE2T and RORA via competitive binding assays, mutation analysis of the interaction interface, or the use of blocking peptides. Third, although current evidence in our work and others demonstrated the ability of UBE2T to ubiquitinate their substrates without the existence of ubiquitin ligase E3, further evidence should be provided to illustrate this issue in our future work.

In summary, our study identified the aberrantly high UBE2T expression in early- stage LUAD was associated with poor outcome, suggesting its potential as a prognostic marker. Further, we partially elucidated the underlying molecular mechanism of the UBE2T-PBX1-RORA signaling pathway in LUAD. Although we have observed that UBE2T directly binds to PBX1 and participates in ubiquitination, whether it relies on classic UBE3 in ubiquitinating PBX1 is still worthy of further investigation.

Abbreviations

CCK-8	Cell Counting Kit-8 assay
ChIP	Chromatin immunoprecipitation
Co-IP	Co-immunoprecipitation
DEGs	Differentially expressed genes
EMT	Epithelial-mesenchymal transition
FAN	Fanconi anemia
GEO	Gene expression omnibus
HPA	Human protein atlas
HR	Hazard ratio
IHC	Immunohistochemistry
LUAD	Lung adenocarcinoma
NSCLC	Non-small cell lung cancer
OS	Overall survival
PBX1	Pre-B-cell leukemia transcription factor 1
PGP	Predominant growth pattern
RORA	Retinoic Acid Receptor-Related Orphan Receptor A
TCGA	The Cancer Genome Atlas
TMA	Tissue microarrays
UBE2T	Ubiquitin Conjugating Enzyme 2 T

Supplementary Information

The online version contains supplementary material available at https://doi.org/10.1186/s12885-024-12887-2.

Supplementary Material 1. Figure S1. GSEA analysis of UBE2T. A. Cell cycle (NES=2.299, NOM *p*-val < 0.0001, FDR<0.0001). B. Proteasome (NES=2.183, NOM *p*-val < 0.0001, FDR=0.002). C. Basal transcription factors (NES=2.145, NOM *p*-val < 0.0001, FDR=0.003). D. Oxidative phosphorylation (NES=1.956, NOM *p*-val = 0.002, FDR=0.015). E. Ubiquitin proteolysis (NES=1.716, NOM *p*-val = 0.036, FDR=0.058). Figure S2. Bioinformatic analyses of UBE2T in different stages of LUAD and its correlation with immune cells. A. UBE2T expression in LUAD with various clinical stages; B. UBE2T expression in LUAD with various pathological stages; C. Forrest plot of UBE2T expression with clinicopathological parameters; D. Correlation of UBE2T expression with infiltration of immune cells. Figure 6S. UBE2T promoted the malignant biological behavior of LUAD cells through the downstream effector RORA (*in vitro*). A. Relative expression of RORA following shUBE2T/OE-UBE2T alone or in combination with RORA-knockdown or overexpression. B-C. Effects of UBE2T combined with RORA

on the proliferation ability assessed by clone formation assay (B) and CCK-8 assay (C). D. Effects of UBE2T combined with RORA on transwell Assay of LUAD cells (10×). E. Detection of EMT downstream target genes affects by UBE2T combined with RORA using Western blot. *p< 0.05, **p < 0.01, ***p < 0.001, as compared with NC group; #p < 0.05, ## p < 0.01, as compared with shUBE2T or UBE2T group, respectively. Table S1 The down-regulated DEGs in OE-UBE2T group (|log2FoldChange| > 1.5, p-value < 0.001). Table S2 The primer sequences for the target genes. Table S3 The association between UBE2T and RORA expression in the 43 stage I LUAD patients. Table S4 The 43 stage I LUAD patients characteristics and the association between UBE2T expression and clinicopathological features. Table S5 Univariate and Multivariate Cox Regression analyses for overall survival in stage I LUAD patients. Table S6 The binding site prediction and primers sequence of PBX1 targeting RORA promoters. Supplementary WB Dataset File. Supplementary Excel 1 DESeqDown-UBE2T overexpression NC_LV5_vs_UBE2T. Supplementary Excel 2 Statistical data for cancer and adjacent tissues IHC. Supplementary Excel 3 CHOICE_Study_Tumor_Adjacent_RNA-seq_Data. Supplementary cell lines STR File.

Acknowledgements
The study protocol was approved by the Human Ethics Review Committee of Fujian Medical University Cancer Hospital (SQ2021-101-01), and a signed informed consent was obtained from each patient. All methods related to animals are reported in accordance with ARRIVE guidelines (https://arrive-guidelines.org) for the reporting of animal experiments and a table of Animal Experimental Ethical Inspection (No.: IACUC FJMU 2022-0475) was obtained from FJMU.

Authors' contributions
Conceptualization and original draft preparation: YJD, XHC and RXZ; Funding acquisition, and supervision: ZGZ, LL, JS, and RXZ; Methodology: XHC, CZH; Investigation: YJD, XRW, JMW, and ZGX; Data analysis: YJD and XHC; Writing and reviewing the manuscript: All authors.

Funding
This study was supported in part by*Fujian Education and Research Grants for Young and Middle-aged Teachers* (Grant No: JAT220083, to Y. Deng), *Foundation Sponsored by Fujian Medical University Cancer Hospital, Fujian Cancer Hospital* (Grant No: 2021YN12, to X. Chen), *Joint Funds for the Innovation of Science and Technology,Fujian Province* (Grant No: 2020Y9036 to X. Chen), *Fujian Research and Training Grants for Young and Middle-aged Leaders in Healthcare* (to X. Chen), *Fujian Provincial Natural and Scientific Foundation* (Grant No: 2023J011255, to X. Chen) *and Financial Special Projects in Form of Research Projects Applied by Fujian Medical University from Fujian Provincial Department of Finance* (Grant No.: 3000–12005103, to R. Zhou).

Availability of data and materials
The datasets generated and/or analyzed during the current study are available from the corresponding author upon reasonable request. The names of the repository/repositories and accession number(s) are available in the: Kaplan–Meier plotter [Lung] (kmplot.com) (223229_at UBE2T), https://portal.gdc.cancer.gov (tumor_stage.diagnoses: Stage-Ia / i Lung adenocarcinoma, LUAD), ChEA3 (maayanlab.cloud), and GEPIA (cancer-pku.cn), GTEx, lung.

Declarations

Ethics approval and consent to participate
This study was carried out in accordance with the ethical guidelines of the 1975 Declaration of Helsinki and was approved by the ethics committee of Fujian Medical university (IACUC FJMU 2022-0475) and the Fujian Cancer Hospital (SQ2021-101-01). Written informed consent was obtained from all patients for the use of the medical records for research purposes.

Consent for publication
Not applicable.

Competing interests
The authors declare no competing interests.

Author details
[1]Department of Medical Oncology, The First Affiliated Hospital of Fujian Medical University, , Fuzhou, Fujian Province 350005, China. [2]Key Laboratory of Gastrointestinal Cancer, Ministry of Education, Fujian Medical University, Fuzhou, Fujian Province 350108, China. [3]School of Basic Medical Sciences, Fujian Medical University, No. 1 Xueyuan Road, Fuzhou, Fujian 350108, China. [4]Department of Thoracic Surgery, Clinical Oncology School of Fujian Medical University, Fujian Cancer Hospital, Fuzhou, Fujian Province 350014, China. [5]Laboratory of Immuno-Oncology, Clinical Oncology School of Fujian Medical University, Fujian Cancer Hospital, 420 Fuma Rd. Jin'an District, Fuzhou, Fujian Province 350014, China.

Received: 12 January 2024 Accepted: 2 September 2024
Published online: 18 September 2024

References

1. Chen W, Zheng R, Baade PD, Zhang S, Zeng H, Bray F, Jemal A, Yu XQ, He J. Cancer statistics in China, 2015. CA Cancer J Clin. 2016;66(2):115–32.
2. Kratzer TB, Bandi P, Freedman ND, Smith RA, Travis WD, Jemal A, Siegel RL. Lung cancer statistics, 2023. Cancer. 2024;130(8):1330–48.
3. Siegel RL, Giaquinto AN, Jemal A. Cancer statistics, 2024. CA Cancer J Clin. 2024;74(1):12–49.
4. Deng Y, Chen X, Huang C, Song J, Feng S, Chen X, Zhou R. Screening and validation of significant genes with poor prognosis in pathologic stage-I lung adenocarcinoma. J Oncol. 2022;2022:3794021.
5. Qin Y, Du J, Fan C. Ube2S regulates Wnt/beta-catenin signaling and promotes the progression of non-small cell lung cancer. Int J Med Sci. 2020;17(2):274–9.
6. Wu Y, Jin D, Wang X, Du J, Di W, An J, Shao C, Guo J. UBE2C induces cisplatin resistance via ZEB1/2-dependent upregulation of ABCG2 and ERCC1 in NSCLC cells. J Oncol. 2019;2019:8607859.
7. Li L, Kang J, Zhang W, Cai L, Wang S, Liang Y, Jiang Y, Liu X, Zhang Y, Ruan H, et al. Validation of NEDD8-conjugating enzyme UBC12 as a new therapeutic target in lung cancer. EBioMedicine. 2019;45:81–91.
8. Ren X, Li A, Ying E, Fang J, Li M, Yu J. Upregulation of ubiquitin-conjugating enzyme E2T (UBE2T) predicts poor prognosis and promotes hepatocellular carcinoma progression. Bioengineered. 2021;12(1):1530–42.
9. Machida YJ, Machida Y, Chen Y, Gurtan AM, Kupfer GM, D'Andrea AD, Dutta A. UBE2T is the E2 in the Fanconi anemia pathway and undergoes negative autoregulation. Mol Cell. 2006;23(4):589–96.
10. Alpi A, Langevin F, Mosedale G, Machida YJ, Dutta A, Patel KJ. UBE2T, the Fanconi anemia core complex, and FANCD2 are recruited independently to chromatin: a basis for the regulation of FANCD2 monoubiquitination. Mol Cell Biol. 2007;27(24):8421–30.
11. Yu Y, Zhu T. RAR-related orphan receptor: an accelerated preeclampsia progression by activating the JAK/STAT3 pathway. Yonsei Med J. 2022;63(6):554–63.
12. Zou Y, Sun H, Guo Y, Shi Y, Jiang Z, Huang J, Li L, Jiang F, Lin Z, Wu J, et al. Integrative pan-cancer analysis reveals decreased melatonergic gene expression in carcinogenesis and RORA as a prognostic marker for hepatocellular carcinoma. Front Oncol. 2021;11:643983.
13. Popov VM, Wang C, Shirley LA, Rosenberg A, Li S, Nevalainen M, Fu M, Pestell RG. The functional significance of nuclear receptor acetylation. Steroids. 2007;72(2):221–30.
14. Yoshida Y, Fukuda T, Tanihara T, Nishikawa N, Iwasa S, Adachi S, Zaitsu O, Terada Y, Tsukamoto R, Shimoshikiryo H, et al. Circadian rhythms in CYP2A5 expression underlie the time-dependent effect of tegafur on breast cancer. Biochem Biophys Res Commun. 2024;708:149813.
15. Li F, Zhang M, Yin X, Zhang W, Li H, Gao C. Exosomes-derived miR-548am-5p promotes colorectal cancer progression. Cell Mol Biol miR-548am-5p. 2023;69(12):104–10.
16. Li C, He J, Meng F, Wang F, Sun H, Zhang H, Dong L, Zhang M, Xu Q, Liang L, et al. Nuclear localization of TET2 requires beta-catenin activation and correlates with favourable prognosis in colorectal cancer. Cell Death Dis. 2023;14(8):552.
17. Li Z, Cui Y, Zhang S, Xu J, Shao J, Chen H, Chen J, Wang S, Zeng M, Zhang H, et al. Novel hypoxia-related gene signature for predicting prognoses that correlate with the tumor immune microenvironment in NSCLC. Front Genet. 2023;14:1115308.

18. Liu L, Guo NA, Li X, Xu Q, He R, Cheng L, Dang C, Bai X, Bai Y, Wang X, et al. miR-125b reverses cisplatin resistance by regulating autophagy via targeting RORA/BNIP3L axis in lung adenocarcinoma. Oncol Res. 2024;32(4):643–58.
19. Zheng J, Deng Y, Huang B, Chen X. Prognostic implications of STK11 with different mutation status and its relationship with tumor-infiltrating immune cells in non-small cell lung cancer. Front Immunol. 2024;15:1387896.
20. Remmele W, Stegner HE. Recommendation for uniform definition of an immunoreactive score (IRS) for immunohistochemical estrogen receptor detection (ER-ICA) in breast cancer tissue. Pathologe. 1987;8(3):138–40.
21. Camp RL, Dolled-Filhart M, Rimm DL. X-tile: a new bio-informatics tool for biomarker assessment and outcome-based cut-point optimization. Clin Cancer Res. 2004;10(21):7252–9.
22. Deshaies RJ. Proteotoxic crisis, the ubiquitin-proteasome system, and cancer therapy. BMC Biol. 2014;12:94.
23. Pu J, Wang B, Zhang D, Wang K, Yang Z, Zhu P, Song Q. UBE2T mediates SORBS3 ubiquitination to enhance IL-6/STAT3 signaling and promote lung adenocarcinoma progression. J Biochem Mol Toxicol. 2024;38(6):e23743.
24. Cai F, Xu H, Song S, Wang G, Zhang Y, Qian J, Xu L. Knockdown of ubiquitin-conjugating enzyme E2 T abolishes the progression of head and neck squamous cell carcinoma by inhibiting NF-Kappab signaling and inducing ferroptosis. Curr Protein Pept Sci. 2024;25:577.
25. Wang Y, Gao G, Wei X, Zhang Y, Yu J. UBE2T Promotes Temozolomide Resistance of Glioblastoma Through Regulating the Wnt/beta-Catenin Signaling Pathway. Drug Des Devel Ther. 2023;17:1357–69.
26. Zhang Y, Yu W, Zhou S, Xiao J, Zhang X, Yang H, Zhang J. Finding key genes (UBE2T, KIF4A, CDCA3, and CDCA5) co-expressed in hepatitis, cirrhosis and hepatocellular carcinoma based on multiple bioinformatics techniques. BMC Gastroenterol. 2024;24(1):205.
27. Li L, Liu J, Huang W. E2F5 promotes proliferation and invasion of gastric cancer through directly upregulating UBE2T transcription. Dig Liver Dis. 2022;54(7):937–45.
28. Huang W, Huang H, Xiao Y, Wang L, Zhang T, Fang X, Xia X. UBE2T is upregulated, predicts poor prognosis, and promotes cell proliferation and invasion by promoting epithelial-mesenchymal transition via inhibiting autophagy in an AKT/mTOR dependent manner in ovarian cancer. Cell Cycle. 2022;21(8):780–91.
29. Qiao L, Dong C, Ma B. UBE2T promotes proliferation, invasion and glycolysis of breast cancer cells by regualting the PI3K/AKT signaling pathway. J Recept Signal Transduct Res. 2022;42(2):151–9.
30. Zhu Y, Liang L, Zhao Y, Li J, Zeng J, Yuan Y, Li N, Wu L. CircNUP50 is a novel therapeutic target that promotes cisplatin resistance in ovarian cancer by modulating p53 ubiquitination. J Nanobiotechnology. 2024;22(1):35.
31. Tao X, Wu X, Zhou P, Yu X, Zhao C, Peng X, Zhang K, Shen L, Peng J, Yang L. UBE2T promotes glioblastoma malignancy through ubiquitination-mediated degradation of RPL6. Cancer Sci. 2023;114(2):521–32.
32. Wang L, Zhang Z, Tian H. Hsa_circ_0092887 targeting miR-490-5p/UBE2T promotes paclitaxel resistance in non-small cell lung cancer. J Clin Lab Anal. 2023;37(1):e24781.
33. Pu J, Zhang D, Wang B, Zhu P, Yang W, Wang K, Yang Z, Song Q. FOXA1/UBE2T inhibits CD8(+)T cell activity by inducing mediates glycolysis in lung adenocarcinoma. Front Biosci (Landmark Ed). 2024;29(4):134.
34. Li Y, Yang X, Lu D. Knockdown of ubiquitin-conjugating enzyme E2T (UBE2T) suppresses lung adenocarcinoma progression via targeting fibulin-5 (FBLN5). Bioengineered. 2022;13(5):11867–80.
35. Zhu J, Ao H, Liu M, Cao K, Ma J. UBE2T promotes autophagy via the p53/AMPK/mTOR signaling pathway in lung adenocarcinoma. J Transl Med. 2021;19(1):374.
36. Yin H, Wang X, Zhang X, Zeng Y, Xu Q, Wang W, Zhou F, Zhou Y. UBE2T promotes radiation resistance in non-small cell lung cancer via inducing epithelial-mesenchymal transition and the ubiquitination-mediated FOXO1 degradation. Cancer Lett. 2020;494:121–31.
37. Anantharajan J, Tan QW, Fulwood J, Sifang W, Huang Q, Ng HQ, Koh X, Xu W, Cherian J, Baburajendran N, et al. Identification and characterization of inhibitors covalently modifying catalytic cysteine of UBE2T and blocking ubiquitin transfer. Biochem Biophys Res Commun. 2023;689:149238.
38. Yu Z, Jiang X, Qin L, Deng H, Wang J, Ren W, Li H, Zhao L, Liu H, Yan H, et al. A novel UBE2T inhibitor suppresses Wnt/beta-catenin signaling hyperactivation and gastric cancer progression by blocking RACK1 ubiquitination. Oncogene. 2021;40(5):1027–42.
39. Sun Y, Lin P, Zhou X, Ren Y, He Y, Liang J, Zhu Z, Xu X, Mao X. TRIM26 promotes non-small cell lung cancer survival by inducing PBX1 degradation. Int J Biol Sci. 2023;19(9):2803–16.
40. Mary L, Leclerc D, Gilot D, Belaud-Rotureau MA, Jaillard S. The TALE never ends: A comprehensive overview of the role of PBX1, a TALE transcription factor, in human developmental defects. Hum Mutat. 2022;43(9):1125–48.
41. Kao TW, Chen HH, Lin J, Wang TL, Shen YA. PBX1 as a novel master regulator in cancer: Its regulation, molecular biology, and therapeutic applications. Biochim Biophys Acta Rev Cancer. 2024;1879(2):189085.
42. Liu Y, Xu X, Lin P, He Y, Zhang Y, Cao B, Zhang Z, Sethi G, Liu J, Zhou X, et al. Inhibition of the deubiquitinase USP9x induces pre-B cell homeobox 1 (PBX1) degradation and thereby stimulates prostate cancer cell apoptosis. J Biol Chem. 2019;294(12):4572–82.
43. Bruckmann C, Tamburri S, De Lorenzi V, Doti N, Monti A, Mathiasen L, Cattaneo A, Ruvo M, Bachi A, Blasi F. Mapping the native interaction surfaces of PREP1 with PBX1 by cross-linking mass-spectrometry and mutagenesis. Sci Rep. 2020;10(1):16809.
44. Du J, Xu R. RORalpha, a potential tumor suppressor and therapeutic target of breast cancer. Int J Mol Sci. 2012;13(12):15755–66.
45. Huang JL, Fu YP, Gan W, Liu G, Zhou PY, Zhou C, Sun BY, Guan RY, Zhou J, Fan J, et al. Hepatic stellate cells promote the progression of hepatocellular carcinoma through microRNA-1246-RORalpha-Wnt/beta-Catenin axis. Cancer Lett. 2020;476:140–51.
46. Lee JM, Kim IS, Kim H, Lee JS, Kim K, Yim HY, Jeong J, Kim JH, Kim JY, Lee H, et al. RORalpha attenuates Wnt/beta-catenin signaling by PKCalpha-dependent phosphorylation in colon cancer. Mol Cell. 2010;37(2):183–95.
47. Leris AC, Roberts TR, Jiang WG, Newbold RF, Mokbel K. WNT5A expression in human breast cancer. Anticancer Res. 2005;25(2A):731–4.
48. Dai B, Fan M, Yu R, Su Q, Wang B, Yang T, Liu F, Zhang Y. Novel diphenyl urea derivative serves as an inhibitor on human lung cancer cell migration by disrupting EMT via Wnt/beta-catenin and PI3K/Akt signaling. Toxicol In Vitro. 2020;69:105000.

Publisher's Note